

Supplementary Materials

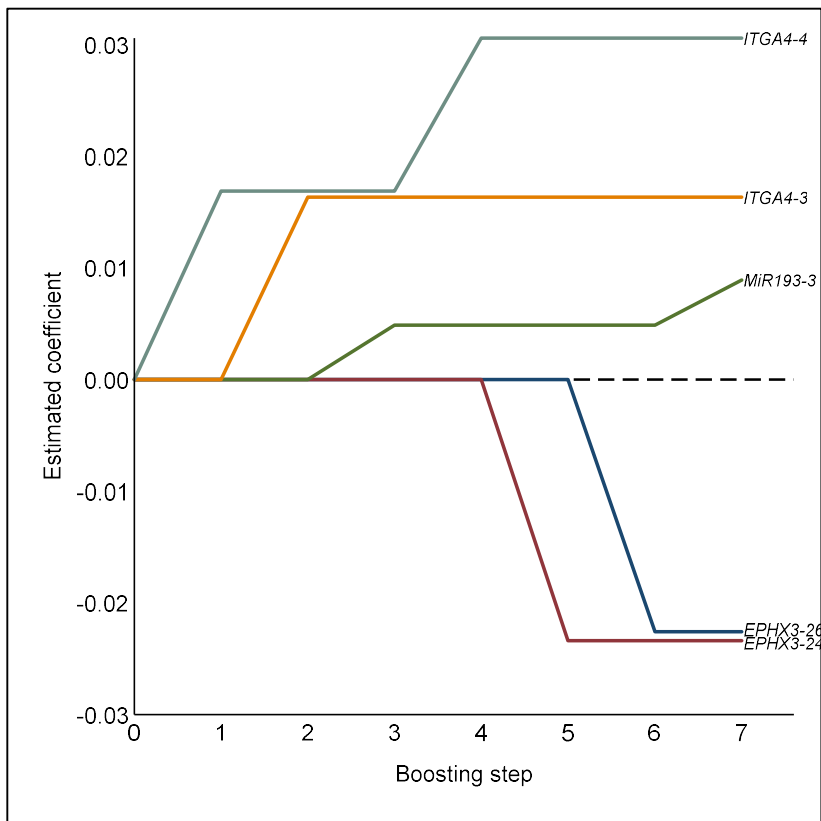


Figure 1. Coefficient paths of the five CpG sites included in the final Cox proportional hazards model. The coefficient estimates are plotted against the boosting steps as obtained from the likelihood-based component-wise algorithm. Coefficients are scaled to be at the level of the original methylation Beta-values.

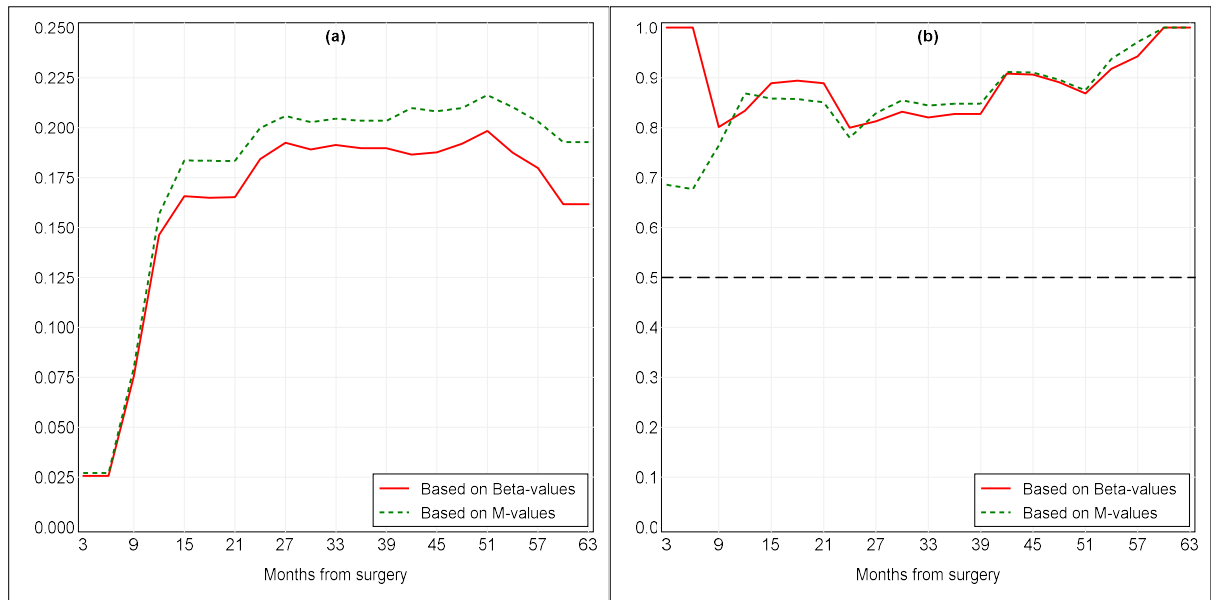


Figure S2. Time-dependent Brier score (a) and area under the receiver operator characteristic curve (AUC) (b) for the final Cox proportional hazards model fitted by component-wise likelihood-based boosting. The dashed line represents a non-discriminatory model (random guessing). M-values were computed as the binary logarithm of the intensities of methylated probes versus non-methylated probes. Performance and predictive accuracy of the model were estimated using the original training set of 36 patients.

Table S1. Permutation-based *P*-value estimations for all candidate methylation data (238 CpG sites). Covariates are ordered from smallest to largest *P*-value.

CpG site	<i>P</i> -value	CpG site	<i>P</i> -value	CpG site	<i>P</i> -value
<i>ITGA4-4</i>	0.0027	<i>PARP15-1</i>	0.4634	<i>GP1BB-7</i>	0.7680
<i>ITGA4-3</i>	0.0078	<i>PARP15-15</i>	0.4635	<i>KIF1A-6</i>	0.7686
<i>MiR193-3</i>	0.0099	<i>EPHX3-29</i>	0.4638	<i>KIF1A-20</i>	0.7732
<i>EPHX3-24</i>	0.0157	<i>MiR193-18</i>	0.4720	<i>MiR296-3</i>	0.7737
<i>EPHX3-26</i>	0.0172	<i>LRRTM1-10</i>	0.4733	<i>LINC0059-2</i>	0.7751
<i>EPHX3-23</i>	0.0196	<i>MiR296-7</i>	0.4804	<i>LRRTM1-18</i>	0.7780
<i>ITGA4-1</i>	0.0234	<i>MiR193-22</i>	0.4821	<i>KIF1A-3</i>	0.7864
<i>EPHX3-18</i>	0.0240	<i>PARP15-19</i>	0.4854	<i>LINC0059-19</i>	0.7889
<i>EPHX3-20</i>	0.0268	<i>ZAP70-9</i>	0.4887	<i>MiR296-13</i>	0.7965
<i>MiR296-10</i>	0.0286	<i>TERT-5</i>	0.5093	<i>NTM-15</i>	0.8033
<i>TERT-2</i>	0.0326	<i>EPHX3-7</i>	0.5105	<i>LRRTM1-16</i>	0.8086
<i>ITGA4-2</i>	0.0350	<i>GP1BB-3</i>	0.5157	<i>KIF1A-14</i>	0.8093
<i>ITGA4-5</i>	0.0404	<i>NTM-4</i>	0.5166	<i>LRRTM1-21</i>	0.8108
<i>ITGA4-9</i>	0.0411	<i>NTM-5</i>	0.5187	<i>KIF1A-26</i>	0.8114
<i>EPHX3-21</i>	0.0427	<i>ZAP70-17</i>	0.5277	<i>LINC0059-4</i>	0.8136
<i>ITGA4-7</i>	0.0451	<i>ZAP70-14</i>	0.5418	<i>LRRTM1-8</i>	0.8177
<i>EPHX3-12</i>	0.0455	<i>GP1BB-17</i>	0.5450	<i>PARP15-3</i>	0.8233
<i>EPHX3-17</i>	0.0476	<i>MiR296-15</i>	0.5481	<i>LRRTM1-1</i>	0.8245
<i>EPHX3-16</i>	0.0495	<i>LRRTM1-3</i>	0.5496	<i>PARP15-17</i>	0.8251
<i>ITGA4-6</i>	0.0511	<i>NTM-14</i>	0.5572	<i>KIF1A-22</i>	0.8268
<i>TERT-1</i>	0.0555	<i>ZAP70-15</i>	0.5578	<i>MiR296-12</i>	0.8280
<i>ITGA4-8</i>	0.0578	<i>PARP15-9</i>	0.5698	<i>LRRTM1-22</i>	0.8301
<i>EPHX3-25</i>	0.0629	<i>MiR193-25</i>	0.5704	<i>KIF1A-12</i>	0.8306
<i>MiR296-14</i>	0.0747	<i>NTM-11</i>	0.5734	<i>MiR193-8</i>	0.8331
<i>EPHX3-4</i>	0.0766	<i>NTM-3</i>	0.5735	<i>LRRTM1-17</i>	0.8351
<i>ITGA4-12</i>	0.0800	<i>GP1BB-8</i>	0.5813	<i>LRRTM1-19</i>	0.8377
<i>MiR296-9</i>	0.0831	<i>TERT-3</i>	0.5829	<i>KIF1A-8</i>	0.8411
<i>EPHX3-14</i>	0.0878	<i>ZAP70-18</i>	0.5844	<i>MiR193-4</i>	0.8419
<i>ITGA4-11</i>	0.0888	<i>ZAP70-8</i>	0.5846	<i>MiR193-24</i>	0.8423
<i>ITGA4-10</i>	0.0921	<i>PARP15-5</i>	0.5849	<i>LINC0059-7</i>	0.8429
<i>EPHX3-22</i>	0.0947	<i>GP1BB-12</i>	0.5884	<i>MiR193-19</i>	0.8432
<i>EPHX3-28</i>	0.1005	<i>GP1BB-11</i>	0.5920	<i>MiR193-5</i>	0.8452
<i>EPHX3-2</i>	0.1084	<i>MiR296-6</i>	0.5962	<i>LINC0059-15</i>	0.8499
<i>ITGA4-14</i>	0.1151	<i>ZAP70-11</i>	0.5963	<i>KIF1A-23</i>	0.8525
<i>EPHX3-5</i>	0.1257	<i>LRRTM1-2</i>	0.6014	<i>TERT-4</i>	0.8543
<i>GP1BB-18</i>	0.1270	<i>ZAP70-12</i>	0.6058	<i>MiR193-11</i>	0.8573
<i>EPHX3-10</i>	0.1311	<i>PARP15-13</i>	0.6058	<i>LINC0059-13</i>	0.8635
<i>ITGA4-13</i>	0.1439	<i>LRRTM1-11</i>	0.6077	<i>KIF1A-25</i>	0.8646
<i>EPHX3-15</i>	0.1526	<i>NTM-12</i>	0.6098	<i>LRRTM1-4</i>	0.8683
<i>EPHX3-13</i>	0.1570	<i>NTM-10</i>	0.6101	<i>LINC0059-3</i>	0.8739
<i>FLI1-4</i>	0.1646	<i>GP1BB-13</i>	0.6184	<i>KIF1A-27</i>	0.8751
<i>EPHX3-8</i>	0.1838	<i>NTM-1</i>	0.6185	<i>MiR193-14</i>	0.8755
<i>EPHX3-11</i>	0.1859	<i>MiR296-1</i>	0.6238	<i>MiR193-17</i>	0.8756
<i>EPHX3-3</i>	0.1942	<i>PARP15-6</i>	0.6246	<i>LINC0059-6</i>	0.8822
<i>ZAP70-3</i>	0.2019	<i>PARP15-10</i>	0.6255	<i>KIF1A-1</i>	0.8872
<i>MiR296-8</i>	0.2043	<i>GP1BB-4</i>	0.6269	<i>LINC0059-16</i>	0.8888
<i>FLI1-5</i>	0.2044	<i>MiR193-23</i>	0.6295	<i>MiR193-21</i>	0.8938
<i>ZAP70-1</i>	0.2079	<i>LRRTM1-13</i>	0.6313	<i>LINC0059-14</i>	0.8938
<i>GP1BB-15</i>	0.2102	<i>NTM-9</i>	0.6337	<i>LRRTM1-20</i>	0.8959
<i>EPHX3-6</i>	0.2151	<i>GP1BB-5</i>	0.6341	<i>TERT-6</i>	0.8997
<i>FLI1-8</i>	0.2152	<i>MiR193-20</i>	0.6383	<i>PARP15-12</i>	0.9038

<i>EPHX3-1</i>	0.2245	<i>NTM-13</i>	0.6433	<i>MiR193-12</i>	0.9053
<i>EPHX3-19</i>	0.2249	<i>MiR193-26</i>	0.6471	<i>LRRTM1-9</i>	0.9065
<i>MiR193-1</i>	0.2291	<i>GP1BB-9</i>	0.6609	<i>PARP15-4</i>	0.9077
<i>MiR193-2</i>	0.2408	<i>GP1BB-10</i>	0.6669	<i>KIF1A-19</i>	0.9104
<i>ZAP70-4</i>	0.2448	<i>MiR296-4</i>	0.6688	<i>KIF1A-11</i>	0.9121
<i>ZAP70-20</i>	0.2449	<i>NTM-7</i>	0.6735	<i>LINC0059-9</i>	0.9164
<i>GP1BB-1</i>	0.2457	<i>GP1BB-6</i>	0.6745	<i>KIF1A-18</i>	0.9180
<i>FLI1-2</i>	0.2493	<i>LRRTM1-5</i>	0.6773	<i>LRRTM1-15</i>	0.9207
<i>ZAP70-7</i>	0.2696	<i>MiR193-16</i>	0.6790	<i>LINC0059-17</i>	0.9239
<i>ZAP70-5</i>	0.2987	<i>LINC0059-5</i>	0.6813	<i>LRRTM1-14</i>	0.9253
<i>MiR296-5</i>	0.3060	<i>PARP15-18</i>	0.6904	<i>LINC0059-8</i>	0.9267
<i>EPHX3-9</i>	0.3064	<i>ZAP70-10</i>	0.6918	<i>MiR296-2</i>	0.9290
<i>PARP15-8</i>	0.3078	<i>LRRTM1-6</i>	0.7063	<i>LINC0059-11</i>	0.9304
<i>FLI1-3</i>	0.3314	<i>LINC0059-18</i>	0.7180	<i>ZAP70-13</i>	0.9321
<i>ZAP70-2</i>	0.3380	<i>MiR193-9</i>	0.7213	<i>LINC0059-12</i>	0.9366
<i>ZAP70-19</i>	0.3542	<i>KIF1A-16</i>	0.7251	<i>MiR193-6</i>	0.9426
<i>MiR193-7</i>	0.3586	<i>KIF1A-5</i>	0.7267	<i>LINC0059-10</i>	0.9448
<i>FLI1-1</i>	0.3613	<i>MiR193-15</i>	0.7278	<i>KIF1A-15</i>	0.9475
<i>EPHX3-27</i>	0.3950	<i>LRRTM1-12</i>	0.7339	<i>PARP15-7</i>	0.9476
<i>FLI1-7</i>	0.4166	<i>MiR193-13</i>	0.7360	<i>KIF1A-17</i>	0.9559
<i>PARP15-2</i>	0.4192	<i>LINC0059-1</i>	0.7434	<i>LRRTM1-7</i>	0.9565
<i>GP1BB-2</i>	0.4205	<i>KIF1A-2</i>	0.7456	<i>KIF1A-4</i>	0.9586
<i>ZAP70-16</i>	0.4322	<i>PARP15-16</i>	0.7515	<i>KIF1A-10</i>	0.9608
<i>NTM-6</i>	0.4449	<i>PARP15-14</i>	0.7570	<i>KIF1A-24</i>	0.9674
<i>ZAP70-6</i>	0.4470	<i>GP1BB-16</i>	0.7573	<i>KIF1A-21</i>	0.9674
<i>NTM-2</i>	0.4508	<i>KIF1A-9</i>	0.7578	<i>KIF1A-13</i>	0.9689
<i>GP1BB-14</i>	0.4545	<i>NTM-8</i>	0.7583	<i>KIF1A-7</i>	0.9760
<i>MiR296-11</i>	0.4580	<i>PARP15-11</i>	0.7603		
<i>MiR193-10</i>	0.4625	<i>LINC0059-20</i>	0.7622		

Table S2. Cox proportional hazards model resulting from likelihood-based component-wise boosting with no information on connection among same-gene CpG sites (optimal number of steps = 10), and after conversion of Beta-values into M-values (optimal number of steps = 4). Non-zero regression coefficients (ln HR) are presented along with hazard ratios (HRs) and permutation-based *P*-values. Coefficients are scaled to be at the level of the original methylation data.

CpG site	Beta-values, no pathway connection information		M-values*	
	Ln HR	HR	Ln HR	HR
<i>EPHX3-18</i>	.	.	-0.3940	0.6744
<i>EPHX3-23</i>	-0.0195	0.9807	.	.
<i>EPHX3-24</i>	-0.0235	0.9768	.	.
<i>EPHX3-25</i>	.	.	-0.4256	0.6534
<i>ITGA4-4</i>	0.0577	1.0594	0.1884	1.2073
<i>MiR193-3</i>	0.0176	1.0178	0.2192	1.2451
<i>Integrated Brier score</i>	0.089		0.070	
<i>C-index</i>	0.805		0.806	
<i>Integrated AUC</i>	0.847		0.834	

* Pathway connection information had no impact on variable selection.

